THE ASTROPHYSICAL JOURNAL, 313:59–68, 1987 February 1

FUNDAMENTAL PROPERTIES OF ELLIPTICAL GALAXIES[1]

S. DJORGOVSKI[2]
Harvard-Smithsonian Center for Astrophysics and Department of Astronomy, University of California, Berkeley
AND
MARC DAVIS
Department of Astronomy, University of California, Berkeley, and Department of Physics, University of California, Berkeley
Received 1986 May 30; accepted 1986 July 18

ABSTRACT

The global properties of elliptical galaxies, such as luminosity, radius, projected velocity dispersion, projected luminosity, etc., form a two-dimensional family. This "fundamental plane" of elliptical galaxies can be defined in observable terms by the velocity dispersion and mean surface brightness. Its thickness is given at present by the present measurement error bars, and there are no significant indications of nonlinearity (deviation from power laws which define the surface), or higher dimensionality. This is indicative of a strong regularity in the process of galaxy formation. The equations of the plane can be used as new, substantially improved distance indicators for elliptical galaxies. However, all morphological parameters which describe the *shape* of the light distribution (ellipticity, ellipticity gradient, isophotal twist rate, slope of the surface brightness profile), and reflect dynamical anisotropies of stars, are completely independent of this fundamental plane, and thus, the elliptical galaxies are actually a "$2+N$" parameter family. The M/L ratios correlate only with the velocity dispersions and show a small intrinsic scatter, perhaps only $\sim 30\%$, in a luminosity range spanning some four orders of magnitude; this suggests a constant fraction of the dark matter contribution in elliptical galaxies.

Subject headings: cosmology — galaxies: internal motions — galaxies: photometry — galaxies: structure

I. INTRODUCTION

Unlike stars of a given age, galaxies cannot be described as a one-parameter family. Herein lines the problem of the "minimal manifold of galaxies" (Brosche 1973), that is, how many and which physical quantities are necessary and sufficient to describe a family of normal galaxies? Our understanding of the structure, formation, and evolution of galaxies depends on the extensive understanding of important physical variables and regularities (correlations) between them.

Most, but not all, properties of galaxies correlate with luminosity (see Kormendy 1982, and references therein). In almost all cases there is a residual scatter, *not* accountable by the measurement errors, indicative of a presence of "hidden parameters." Examples of this phenomenon are the distance indicator relations, Tully-Fisher for spirals, and Faber-Jackson for the early types. Thus, if the minimal manifold of galaxies is known, one may improve substantially on the mapping of the local large-scale velocity field. Knowledge and understanding of the minimal manifold of galaxies would provide a benchmark for the theories of galaxy formation, and dynamical models of elliptical galaxies.

In this spirit, properties of spirals were investigated by Bujarrabal, Guibert, and Balkowski (1981), Whitmore (1984), and Watanabe, Kodaira, and Okamura (1985), who concluded that two principal quantities are necessary. For the early-type galaxies, most authors agreed that there is more than one important quantity (the one being the luminosity), but there was no clear understanding or agreement as what the second parameter may be; see Tonry and Davis (1981), Terlevich *et al.* (1981), Efstathiou and Fall (1984), Lauer (1985), and finally Burstein *et al.* (1986) and Dressler *et al.* (1986). We exclude from the present discussion diffuse dwarfs, which are probably a completely different family of galaxies (see Wirth and Gallagher 1984; Kormendy 1985; Sandage, Binggeli, and Tamman 1985). We will address here the properties of "classical" ellipticals.

II. THE DATA AND THE METHODS

In order to address this problem, a large and homogeneous data base is necessary. We used morphological parameters, radii, and magnitudes from the CCD surface photometry survey of ~ 260 early-type galaxies by Djorgovski (1985*a*), line strength and central velocity dispersion measurements by Tonry and Davis (1981), and the compilation by Whitmore, McElroy, and Tonry (1985). The details of surface photometry survey, data reductions, error estimates, and calibrations are given by Djorgovski (1985*a*; and in preparation). The composition of the sample, selection of galaxies, and completeness are discussed in that reference; suffice it to say that the selection effects are well understood.

In order to parametrize the morphology of galaxies in the sample, a consistent radial scale is needed. Galaxies have no edges, and there is a problem of standard, or fiducial radii. We feel that a radial scale independent and decoupled from the magnitude or surface brightness calibration is necessary, and thus we reject use of any form of isophotal radii. The total light is not known for most (or all) galaxies, and thus we cannot use the half-light radii. It is thus necessary to derive a radial scale from the surface brightness profiles themselves. One method is to devise dimensionless functions of radius, such as Petrosian's (1976) η-function (see Djorgovski, Davis, and Kent 1985). Several different radial scales were used, and produced very

[1] Based in part on the observations done at Lick Observatory, University of California.
[2] Harvard Junior Fellow.

similar results. In this paper, for the sake of simplicity we use the values of r_e (actually, a semimajor axis, not radius) obtained from the fits of surface brightness to the $r^{1/4}$ formula of de Vaucouleurs outside the innermost 3″, in order to avoid the seeing effects; the outer bound is typically $\sim 1'$ or larger. Our r_e is operationally a parameter from the fit, rather than a half-light radius, and the two would be equal only for a "perfect" $r^{1/4}$ galaxy (there is also an ellipticity term, as we follow the actual shape of the galaxy and do not force circular apertures). All quantities used in the present paper are measured at r_e, or within the elliptical isophote whose semimajor axis is r_e. We emphasize that the results are essentially the same with all radial scales which we used, but slightly better fits are obtained with larger radii: the relations obtained below are robust, but they are indicative of more global, rather than central, properties of galaxies. Other radial scales will be employed in a future paper.

For each galaxy, we thus have measurements of radius, magnitude, mean and local surface brightness, slope of the surface brightness profile, ellipticity, ellipticity gradient, and isophotal twist rate, all measured at or within the r_e elliptical aperture. The magnitudes are defined in appropriate elliptical-isophote apertures; both magnitudes and surface brightness are in the r_G band, defined by Djorgovski (1985*b*). In addition, there are central velocity dispersion (σ) and line strength measurements from the literature, although not for all galaxies in the survey. There are carefully estimated error bars for all quantities, including both the internal errors (e.g., error in radius penetrates into an error in surface brightness, etc.) and the external ones (e.g., magnitude zero-point calibration). After rejection of S0's and the galaxies with no published velocity dispersions, poor photometric calibration, or with data obtained in very bad seeing, we are left with 122 galaxies; out of these, 16 are located in the "triple value zone" of the local velocity field and were omitted from the fits involving distance-dependent quantities. The data used in the present paper (except for some of the shape parameters) are listed in Table 1.

The method of the present investigation is multibivariate statistics: we obtain least-squares fits of two quantities, and then correlate error-rescaled residuals from the fit with other quantities. If residuals correlate with a third quantity, we make a linear combination of that quantity and one of the previous two, and optimize the fit again. For example, if residuals from the best fit in the $L - \sigma$ relation correlate with surface brightness, μ, we make a set of linear combinations of $\log \sigma$ and μ and search for the combination which gives the best fit. The fit quality is judged by following the χ^2 values, linear regression and rank correlation coefficients, and the size of predicted errors in galaxy distances, if the relation is to be used as a distance indicator. The least-squares fits allow properly for errors in both coordinates; this procedure also diminishes the effects of a possible Malmquist bias, if any is present.

For the fits involving radius or luminosity, we used a spherically symmetric, nonlinear Virgocentric infall model, where the infall velocity at any given radius from Virgo is given by

$$V_{\rm INF} = V_{\rm LG} \times \frac{\delta(1 + \delta/3)^{-1/2}}{\delta_0(1 + \delta_0/3)^{-1/2}} \qquad (1)$$

(Meiksin 1985), where $V_{\rm LG}$ is the infall velocity at the Local Group, δ is the overdensity factor within that radius, and $\delta_0 = 2$ is the overdensity factor within the Local Group radius. We also use the values for Virgo cluster center and redshift from Huchra (1985). In the fits we solve simultaneously for the Local Group infall velocity, $V_{\rm LG}$. Introduction of an infall model is required by the fact that many of the galaxies in our sample are members of the Local Supercluster, and considerable errors in distance-dependent quantities can be introduced if the infall components of the observed velocities are not accounted for. Since there are over 100 data points, introduction of another parameter in the fits (the Local Group infall velocity) does not perceptibly compromise the statistics, and, as it turns out, the results described below are not very sensitive to the value of our $V_{\rm INF}$.

This paper is intended to communicate briefly the main results obtained so far. We will present the complete set of data, further details of our statistical analysis and model fitting, an additional multivariate analysis, and the application to the mapping of the local velocity field in a future paper.

III. THE FUNDAMENTAL PLANE, OR THE OPTIMAL DISTANCE-INDICATOR RELATIONS

One way of approaching this problem is by investigating the known distance-indicator relations (luminosity or radius vs. velocity dispersion or surface brightness). It was immediately apparent that the residuals of $L - \sigma$ and $R - \sigma$ relations correlate well with the mean surface brightness ($\langle\mu\rangle$, in the usual logarithmic/magnitude form), and vice versa. On the other hand, σ and $\langle\mu\rangle$ do not correlate at all. This leads us to the solution: linear combinations of $\log \sigma$ and $\langle\mu\rangle$ with $\log L$ or $\log R$ produce excellent fits, with no residual scatter, i.e., not accountable by the measurement errors. This process is illustrated in Figure 1. The new distance-indicator relations, which at the same time are the equations of a plane in the L (or R) $- \sigma - \langle\mu\rangle$ parameter space, are

$$M(r_e) = -8.62(\log \sigma + 0.10\langle\mu\rangle) + 16.14 , \qquad (2a)$$

or

$$L \sim \sigma^{3.45}\langle \mathrm{SB}\rangle^{-0.86} . \qquad (2b)$$

$$\log r_e = 1.39(\log \sigma + 0.26\langle\mu\rangle) - 6.71 , \qquad (3a)$$

or

$$R \sim \sigma^{1.39}\langle \mathrm{SB}\rangle^{-0.90} . \qquad (3b)$$

Here SB denotes surface brightness in linear flux units. These relations supersede those from our preliminary report (Djorgovski and Davis 1986)[3]. The ratios of coefficients multiplying σ and $\langle\mu\rangle$ are uncertain by $\sim 10\%$. These distance-indicator relations represent the fundamental plane viewed edge-on. The equations are derived independently, and thus do not transform into each other exactly. The equations (3a) and (3b) are the better ones, since the magnitude zero-point calibration errors do not affect our measurements of the radii, but they do contribute to the errors of magnitudes used in deriving the equations (2a) and (2b).

The use of these and other relations for the mapping of the local large-scale velocity field will be explored in a forthcoming paper; suffice to say that within our spherically symmetric Virgo infall model, we obtain values of the Local Group infall velocity of ~ 350–400 km s^{-1}, with typical 1 σ errors of ~ 140 km s^{-1}.

A nearly equivalent result was achieved independently by

[3] Note that the powers of surface brightness in the equations stated in that paper are in error, and should be multiplied by 6.25.

TABLE 1

DATA FOR GALAXIES OUTSIDE THE TRIPLE-VALUED ZONE

Galaxy (1)	log(re/") (2)	(3)	log(re/pc) (4)	(5)	m(re) (6)	(7)	M(re) (8)	(9)	<mu>e (10)	(11)	Ell(re) (12)	(13)	log(sigmav) (14)	(15)
NGC 57	1.29	.02	3.70	.02	11.86	.44	-21.76	.44	19.28	.47	0.17	.02	2.502	.025
NGC 97	1.18	.01	3.54	.01	12.44	.16	-20.92	.16	19.55	.17	0.06	.02	2.086	.117
NGC 194	1.40	.01	3.79	.01	11.94	.06	-21.55	.06	20.14	.08	0.11	.02	2.332	.051
NGC 221	1.65	.01	2.16	.05	7.89	.21	-16.21	.31	17.27	.22	0.17	.02	1.898	.055
NGC 410	1.62	.01	4.03	.01	11.26	.30	-22.36	.30	20.37	.32	0.26	.02	2.458	.023
NGC 430	1.05	.08	3.44	.08	12.62	.28	-20.92	.28	18.86	.46	0.30	.02	2.497	.060
NGC 533	1.67	.04	4.09	.04	11.14	.15	-22.52	.15	20.52	.17	0.27	.02	2.471	.021
NGC 584	1.57	.01	3.50	.02	10.33	.16	-20.91	.16	18.90	.17	0.37	.02	2.369	.028
NGC 596	1.35	.01	3.28	.02	11.00	.08	-20.22	.08	18.91	.11	0.10	.02	2.233	.031
NGC 636	1.27	.01	3.20	.02	11.60	.14	-19.61	.14	19.05	.16	0.14	.02	2.238	.030
NGC 661	1.21	.01	3.48	.01	11.92	.16	-21.01	.16	18.96	.18	0.28	.01	2.272	.035
NGC 680	1.24	.01	3.40	.01	11.60	.17	-20.77	.17	18.84	.19	0.20	.02	2.362	.023
NGC 720	1.60	.01	3.51	.02	10.50	.16	-20.61	.16	19.27	.18	0.43	.02	2.350	.049
NGC 741	1.54	.02	3.96	.02	11.31	.14	-22.37	.14	20.20	.16	0.13	.02	2.477	.029
NGC 750	1.91	.06	4.32	.06	10.86	.16	-22.76	.16	21.45	.27	0.21	.14	2.297	.064
NGC 751	2.08	.09	4.50	.09	10.86	.26	-22.79	.26	22.77	.43	0.00	.04	2.369	.060
NGC 777	1.40	.04	3.79	.04	11.30	.15	-22.21	.15	19.51	.22	0.16	.02	2.525	.032
NGC 821	1.56	.01	3.49	.02	10.65	.06	-20.60	.06	19.43	.07	0.28	.02	2.332	.030
NGC 990	1.05	.04	3.29	.04	12.83	.24	-19.92	.24	19.14	.31	0.16	.02	2.260	.053
NGC 1016	1.38	.01	3.88	.01	11.66	.12	-22.42	.12	19.82	.13	0.06	.02	2.479	.019
NGC 1052	1.61	.02	3.48	.02	9.79	.65	-21.13	.65	18.93	.68	0.29	.02	2.310	.032
NGC 1132	1.62	.01	4.15	.01	11.82	.12	-22.38	.12	20.94	.14	0.31	.03	2.394	.025
NGC 1172	1.24	.02	3.15	.03	12.27	.11	-18.85	.11	19.51	.14	0.17	.02	2.299	.026
NGC 1199	1.41	.02	3.53	.02	11.71	.19	-20.46	.19	19.83	.22	0.22	.01	2.322	.027
NGC 1209	1.42	.02	3.53	.02	11.10	.08	-21.00	.08	18.66	.11	0.54	.02	2.412	.025
NGC 1395	1.67	.01	3.61	.01	10.01	.11	-21.25	.11	19.47	.12	0.18	.02	2.396	.056
NGC 1407	1.69	.01	3.65	.01	9.88	.06	-21.48	.06	19.41	.07	0.16	.02	2.438	.019
NGC 1426	1.41	.02	3.28	.02	11.42	.23	-19.49	.23	19.25	.15	0.34	.03	2.196	.042
NGC 1439	1.41	.02	3.35	.02	11.50	.17	-19.74	.17	19.79	.20	0.10	.02	2.270	.047
NGC 1521	1.33	.01	3.64	.01	11.64	.14	-21.49	.14	19.42	.15	0.23	.02	2.326	.054
NGC 1587	1.37	.01	3.64	.01	11.46	.52	-21.48	.52	19.33	.54	0.18	.02	2.360	.051
NGC 1600	2.04	.08	4.41	.08	10.18	.29	-23.25	.29	22.00	.40	0.26	.02	2.509	.027
NGC 1653	1.28	.02	3.63	.02	11.72	.13	-21.57	.13	19.31	.17	0.06	.02	2.442	.063
NGC 1700	1.35	.01	3.65	.01	11.03	.08	-22.04	.08	18.66	.10	0.34	.01	2.369	.037
NGC 2476	1.08	.02	3.40	.02	12.50	.12	-20.68	.12	18.59	.14	0.30	.02	2.276	.053
NGC 2778	1.21	.01	3.34	.02	12.53	.06	-19.67	.06	19.57	.08	0.20	.01	2.274	.035
NGC 2832	1.49	.02	4.05	.02	11.55	.11	-22.81	.11	20.05	.14	0.24	.02	2.483	.021
NGC 2872	1.56	.14	3.84	.14	11.13	.50	-21.82	.50	20.21	.34	0.18	.07	2.473	.029
NGC 3070	1.14	.03	3.61	.03	12.20	.17	-21.69	.17	19.00	.22	0.14	.03	2.382	.016
NGC 3091	1.33	.01	3.63	.01	11.41	.13	-21.68	.13	19.11	.15	0.25	.02	2.408	.055
NGC 3158	1.39	.02	3.94	.02	11.79	.08	-22.56	.08	19.90	.13	0.12	.02	2.563	.024
NGC 3193	1.31	.01	3.34	.02	11.15	.15	-20.56	.15	18.81	.18	0.08	.01	2.265	.043
NGC 3226	1.75	.02	3.75	.03	11.03	.43	-20.58	.43	20.80	.42	0.26	.03	2.316	.053
NGC 3853	1.12	.02	3.41	.02	12.49	.18	-20.54	.18	18.94	.22	0.32	.02	2.246	.047
NGC 3862	0.97	.02	3.51	.02	12.94	.15	-21.30	.15	19.03	.19	0.01	.01	2.412	.037
NGC 4168	1.55	.02	3.39	.02	11.02	.23	-19.76	.23	20.07	.26	0.09	.02	2.260	.024
NGC 4239	1.60	.02	3.44	.04	12.23	.27	-18.55	.27	21.10	.23	0.46	.03	1.740	.080
NGC 4261	1.54	.00	3.69	.02	10.43	.21	-21.92	.21	19.15	.22	0.18	.01	2.530	.026
NGC 4318	1.06	.01	2.91	.02	12.85	.18	-17.93	.18	19.06	.18	0.34	.02	1.991	.049
NGC 4365	1.77	.02	3.61	.02	9.62	.14	-21.16	.14	19.59	.10	0.21	.02	2.418	.020
NGC 4374	1.59	.00	3.43	.01	9.25	.16	-21.53	.16	18.49	.16	0.10	.02	2.471	.022
NGC 4387	1.54	.03	3.38	.05	11.51	.16	-19.27	.17	20.14	.23	0.34	.02	2.045	.039
NGC 4406	1.92	.01	3.76	.11	9.05	.15	-21.73	.19	19.72	.14	0.25	.02	2.408	.025
NGC 4434	1.15	.01	2.99	.03	12.05	.10	-18.73	.10	18.93	.13	0.07	.01	2.057	.057
NGC 4458	1.42	.02	3.26	.04	11.93	.11	-18.85	.12	19.91	.14	0.31	.05	2.000	.088
NGC 4472	1.93	.00	3.77	.01	8.38	.26	-22.40	.26	19.13	.27	0.15	.02	2.498	.028
NGC 4473	1.45	.01	3.29	.01	10.16	.05	-20.62	.05	18.23	.06	0.41	.02	2.294	.044
NGC 4478	1.28	.01	3.12	.02	11.09	.12	-19.69	.12	18.58	.13	0.16	.02	2.158	.030
NGC 4486	2.21	.02	4.05	.02	8.16	.32	-22.62	.32	20.60	.36	0.10	.01	2.525	.032
NGC 4486B	0.26	.02	2.10	.03	14.28	.15	-16.50	.15	16.66	.12	0.19	.02	2.274	.094
NGC 4489	1.62	.02	3.47	.03	11.78	.17	-19.00	.17	21.01	.20	0.16	.02	1.820	.100
NGC 4551	1.70	.04	3.54	.04	11.15	.21	-19.63	.21	20.67	.24	0.31	.02	2.083	.072
NGC 4552	1.41	.00	3.26	.05	9.98	.11	-20.80	.12	18.19	.12	0.09	.02	2.436	.032
NGC 4564	1.69	.02	3.53	.03	10.80	.10	-19.98	.10	19.56	.16	0.54	.02	2.217	.053
NGC 4621	1.64	.01	3.48	.03	9.76	.15	-21.02	.15	18.88	.16	0.36	.02	2.352	.029
NGC 4649	1.84	.01	3.68	.02	8.70	.17	-22.08	.17	18.94	.18	0.24	.01	2.537	.032
NGC 4660	1.31	.02	3.15	.03	10.89	.16	-19.89	.16	18.08	.21	0.46	.01	2.292	.027
NGC 4782	1.79	.01	4.18	.02	10.62	.17	-22.89	.17	20.85	.18	0.31	.03	2.585	.031
NGC 4783	1.63	.02	3.96	.02	11.44	.14	-21.78	.14	20.75	.19	0.23	.02	2.438	.037
NGC 4867	0.73	.03	3.14	.03	14.42	.20	-19.23	.20	19.01	.22	0.18	.02	2.348	.021
NGC 4874	1.66	.02	4.24	.02	11.64	.14	-22.78	.14	21.06	.20	0.16	.02	2.418	.033
NGC 4881	1.04	.02	3.58	.02	13.37	.07	-20.92	.07	19.75	.10	0.06	.02	2.286	.023
NGC 4886	0.89	.03	3.40	.03	14.19	.21	-19.95	.21	19.76	.25	0.04	.01	2.190	.025
NGC 4889	1.59	.01	4.12	.01	11.36	.11	-22.89	.11	20.29	.13	0.29	.02	2.592	.022
NGC 5129	1.48	.18	4.03	.18	12.31	.62	-22.02	.62	20.34	.49	0.33	.03	2.400	.061
NGC 5322	1.64	.01	3.71	.01	10.17	.11	-21.73	.11	19.25	.12	0.31	.02	2.491	.042
NGC 5424	1.25	.03	3.74	.03	12.72	.21	-21.31	.21	19.95	.25	0.24	.02	2.149	.144
NGC 5490	1.25	.00	3.67	.01	12.08	.13	-21.60	.13	19.36	.14	0.20	.02	2.403	.050
NGC 5638	1.62	.00	3.65	.01	10.87	.02	-20.84	.02	20.17	.03	0.09	.01	2.225	.052
NGC 5796	1.32	.01	3.52	.01	11.23	.16	-21.34	.16	18.86	.18	0.17	.02	2.501	.019
NGC 5813	1.43	.02	3.49	.03	10.95	.20	-20.93	.20	19.11	.22	0.19	.02	2.364	.028
NGC 5831	1.34	.01	3.35	.02	11.37	.08	-20.24	.08	19.39	.10	0.11	.02	2.233	.051
NGC 5845	0.58	.01	2.53	.02	12.64	.05	-18.65	.05	16.49	.06	0.24	.02	2.387	.045
NGC 5846B	0.57	.11	2.68	.11	13.69	.28	-18.42	.28	17.48	.40	0.21	.03	2.279	.055

TABLE 1—*Continued*

(1)	(2)	(3)	(4)	(5)	(6)	(7)	(8)	(9)	(10)	(11)	(12)	(13)	(14)	(15)
NGC 5846	1.78	.01	3.79	.02	10.40	.09	−21.24	.09	20.45	.14	0.09	.01	2.398	.026
NGC 5966	1.48	.02	3.85	.03	12.08	.19	−21.36	.19	20.43	.26	0.38	.02	2.250	.059
NGC 5982	1.37	.02	3.58	.02	11.05	.08	−21.59	.08	18.87	.11	0.29	.02	2.394	.026
NGC 6086	1.28	.01	3.95	.01	12.58	.16	−22.33	.16	20.00	.17	0.29	.02	2.509	.035
NGC 6137	1.62	.01	4.29	.01	11.84	.18	−23.05	.18	20.60	.20	0.47	.01	2.453	.035
NGC 6146	1.18	.01	3.82	.01	12.47	.13	−22.30	.13	19.39	.15	0.23	.02	2.364	.068
NGC 6166	2.19	.03	4.85	.03	9.46	.42	−25.42	.42	23.66	.39	0.67	.09	2.480	.043
NGC 6173	1.35	.01	3.99	.01	12.13	.03	−22.64	.03	19.77	.04	0.32	.01	2.336	.073
NGC 7391	1.23	.01	3.36	.01	12.03	.12	−20.23	.12	19.23	.15	0.14	.02	2.481	.066
NGC 7454	1.75	.03	3.71	.03	11.14	.19	−20.24	.19	21.16	.28	0.16	.04	2.134	.042
NGC 7458	1.04	.01	3.40	.01	12.69	.12	−20.67	.12	18.79	.13	0.23	.01	2.167	.171
NGC 7562	1.42	.02	3.64	.02	11.18	.29	−21.47	.29	19.11	.30	0.31	.02	2.459	.045
NGC 7619	1.32	.01	3.57	.01	11.28	.06	−21.51	.06	18.85	.08	0.22	.01	2.519	.026
NGC 7626	1.57	.01	3.76	.01	10.91	.21	−21.63	.21	19.85	.23	0.12	.02	2.431	.032
NGC 7660	1.11	.01	3.55	.01	12.40	.27	−21.33	.27	18.92	.29	0.25	.02	2.320	.080
NGC 7768	1.34	.02	3.93	.02	12.10	.18	−22.41	.18	19.70	.22	0.28	.02	2.560	.023
NGC 7778	1.52	.03	3.90	.03	11.78	.18	−21.72	.18	20.54	.25	0.09	.02	2.322	.108
NGC 7785	1.55	.02	3.80	.02	11.23	.17	−21.57	.17	19.65	.21	0.44	.01	2.382	.045
IC 179	1.15	.01	3.47	.02	12.45	.14	−20.73	.14	19.28	.17	0.16	.02	2.447	.030
IC 962	0.80	.04	3.31	.04	13.24	.22	−20.86	.22	18.31	.28	0.10	.01	2.185	.086
IC 1211	1.10	.02	3.56	.02	12.75	.13	−21.11	.13	19.33	.17	0.13	.01	2.212	.123
IC 4051	0.88	.02	3.30	.02	14.11	.18	−19.58	.18	19.56	.21	0.17	.02	2.362	.017

Col. (1).—Most common name of a galaxy.

Cols. (2), (3).—log r_e (semimajor axis), measured in arc seconds, and its error. See text for more details.

Cols. (4), (5).—log r_e, measured in parsecs, and its error. Virgocentric infall model with $V = 400$ km s^{-1} was assumed.

Cols. (6), (7).—Apparent magnitude, measured within the r_e elliptical isophote, and its error, in the r_G band (Djorgovski 1985*b*).

Cols. (8), (9).—Absolute magnitude, measured within the r_e elliptical isophote, and its error, in the r_G band. Virgocentric infall model with $V = 400$ km s^{-1} was assumed.

Cols. (10), (11).—Mean surface brightness within the r_e elliptical isophote, measured in r_G magnitudes per square arc seconds, and its error.

Cols. (12), (13).—Ellipticity, measured at the r_e isophote, and its error.

Cols. (14), (15).—Logarithm of the central velocity dispersion, measured in km s^{-1}, and its error. Data were taken mostly from Whitmore, McElroy, and Tonry 1985, repeated here for convenience.

Burstein *et al.* (1986) and Dressler *et al.* (1986), who have already applied their solution to the mapping of the large-scale velocity field. Their quantity D_Σ is a mixture of radius and surface brightness terms in our representation, and we have little doubt that the fundamental plane is the same in both cases. Possible significance of surface brightness as the second parameter in the Faber-Jackson relation was already indicated by de Vaucouleurs and Olson (1982), and Lauer (1985) has advocated importance of the central luminosity and claimed two-dimensionality in the core properties of ellipticals.

Introduction of line strength does not improve the fits very much. Line strengths and colors are very well correlated with σ, and should probably be omitted from this discussion. There are, however, very marginal indications that introduction of ellipticity terms reduces slightly the residual scatter in these relations. Beyond that, the residuals of new relations do not correlate with any other morphological or spectroscopic quantity, indicating that two dimensions provide an adequate and exhaustive description of the global properties of ellipticals.

Again, we think that there is nothing "magical" about r_e (in our operational definition), or D_Σ, or any other radial scale, and about equally good results with stable power laws are achieved with any consistently applied radial scale, as long as most of the galaxian light is contained within the apertures of choice. Surface brightness profiles of ellipticals are almost always close to a scale-free power law, and they also show subtle but real differences in shape, without any very obvious systematic. It may be simply impossible to define a "perfect," homogeneous and universal radial scale.

We may ask, how linear are the equations (2a)–(3b), or how flat is the "fundamental plane"? This is an essential question if the new distance-indicator relations are to be used for the determination of peculiar velocities—and Burstein *et al.* (1986) *did* find large peculiar velocities. We do not doubt the importance of their results, but the linearity of these new distance indicators is still not proven on a few percent level, and some spurious contributions to the peculiar velocities are, in principle, still possible. One physical mechanism which may introduce deviations from the plane could be dissipationless mergers, which may afflict the "bright" end. There may be a slight curvature in the L (or R) $-\sigma-\langle\mu\rangle$ relations (see Figs, 1*e*, 1*f*), but any firm conclusion is premature at this point. The plane appears to be flat within the present measurement errors, and any slight curvature should not introduce distance errors larger than $\sim$5%–10%. It is still possible that there are small differences in the tilts and/or intercepts of the fundamental plane in different large-scale environments, reflecting, perhaps, some real fluctuations in the process of galaxy formation (see also Kraan-Korteweg 1983). It is also possible that galaxies in all cluster/field environments lie on the same plane but populate different portions of it. This may be investigated by looking at the distributions perpendicular to the luminosity axis in the plane, thus factoring out any possible differential selection effects.

IV. THE MANIFOLD OF ELLIPTICAL GALAXIES

The plane defined by σ and $\langle\mu\rangle$ (Fig. 2) also defines other global properties of ellipticals, their luminosities, radii, line strengths, and presumably integrated colors. The independence of σ (which conveys the depth of the potential well of a galaxy) and $\langle\mu\rangle$ (which is the projected density of the *luminous* material) is quite remarkable, since both of them correlate separately with the luminosity and radius.

The fundamental plane is remarkably thin–its thickness is completely contained in the present measurement errors, and any "cosmic broadening" must be very small, on the level of a

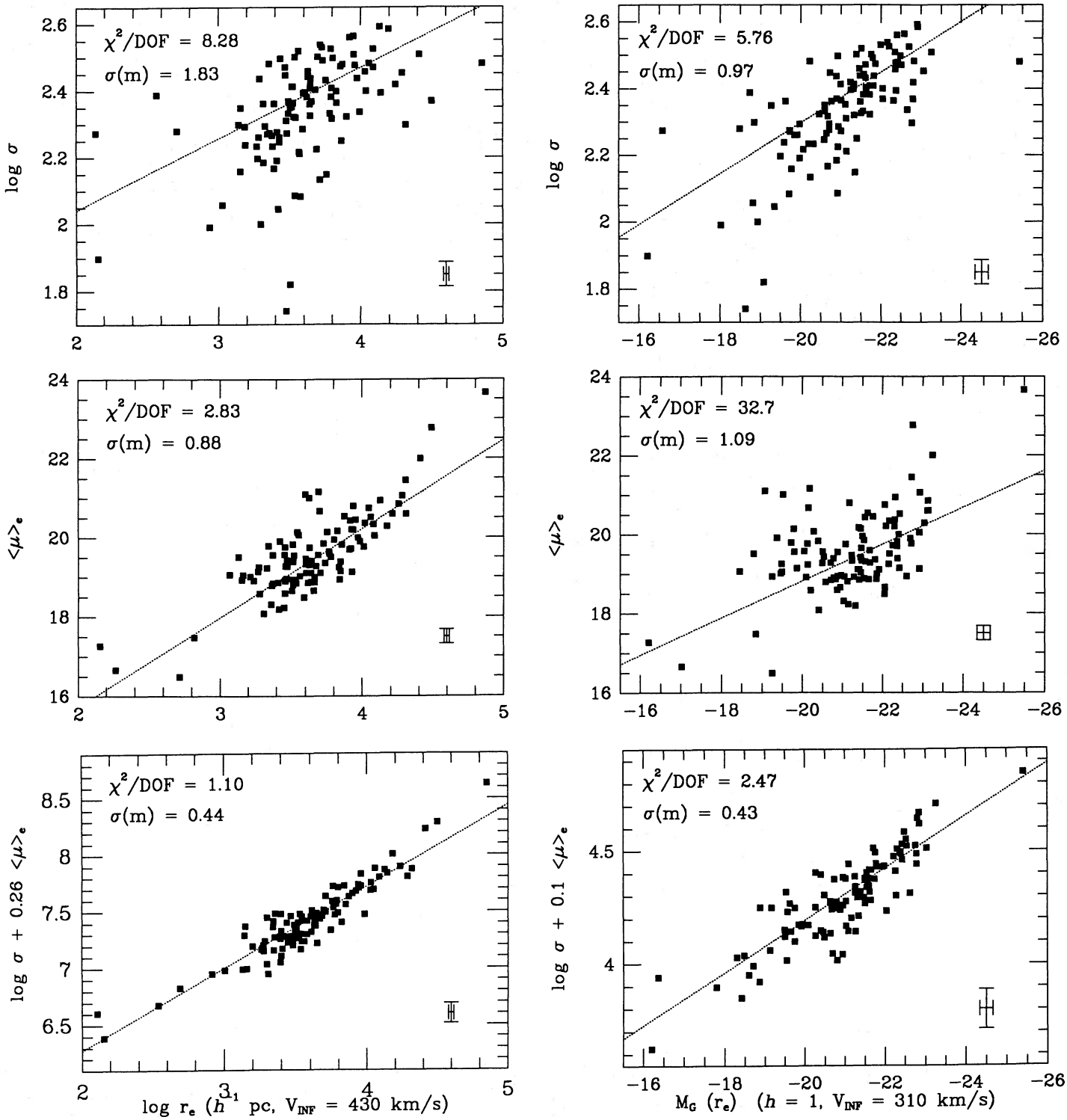

FIG. 1.—The old and the new distance-indicator relations. Correlations with radius are on the left, and with luminosity on the right. *Top row:* correlations with the central projected velocity dispersion, σ. *Middle:* correlations with the mean surface brightness, $\langle\mu\rangle$. *Bottom:* the new distance indicators, given by eqs. (2a), (2b) and (3a), (3b). Dotted lines represent the least-squares fits. Median errors are indicated by the error bars in the lower right corners. Reduced chi-squares, χ^2/DOF, and estimated errors of relations when used as distance predictors, expressed in magnitudes, $\sigma(m)$, are shown in upper left corners. The chi-squares are slightly off, because of the inevitable slight correlations of errors in log r_e and errors in $\langle\mu\rangle$, and the common magnitude zero-point calibration errors in M and $\langle\mu\rangle$.

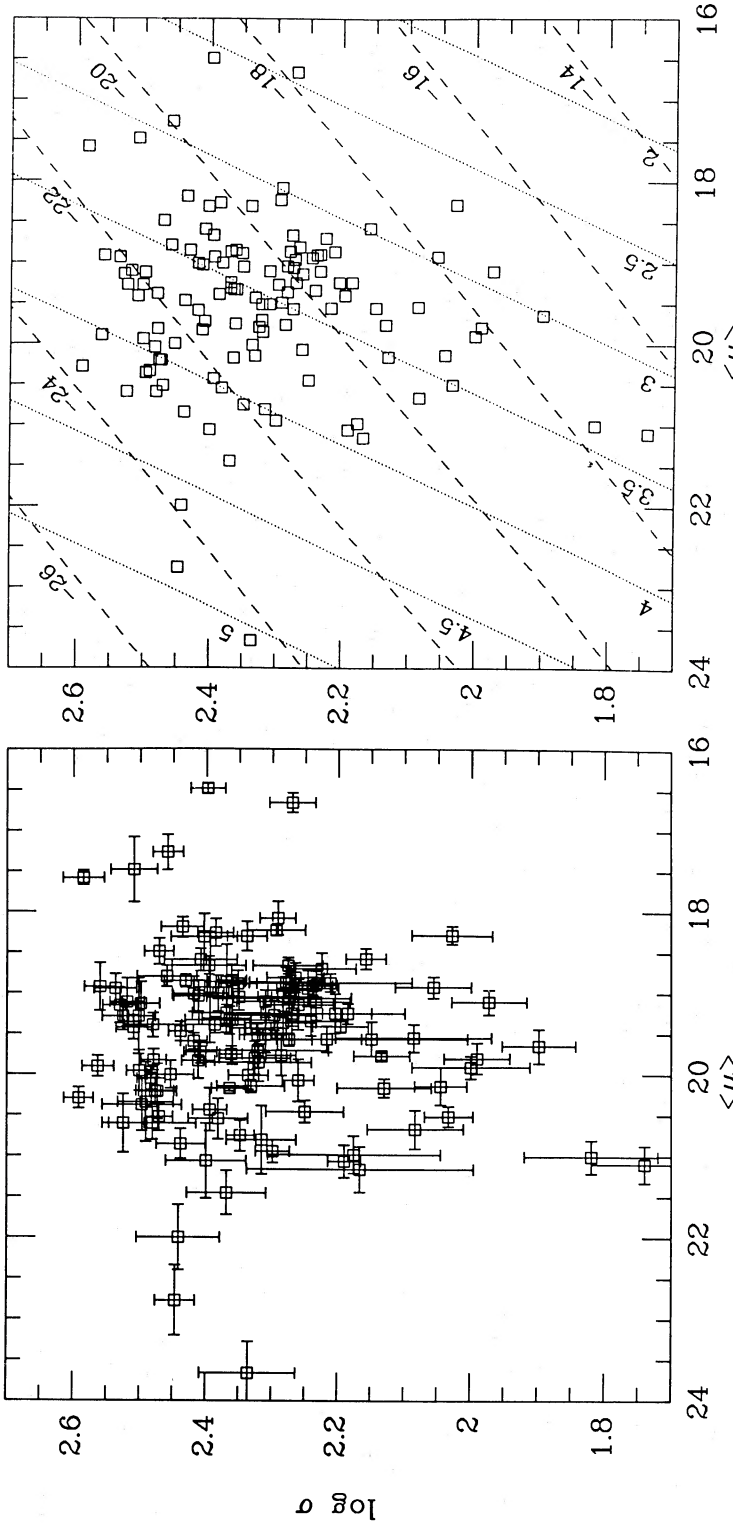

FIG. 2.—Fundamental plane of elliptical galaxies, shown through the observable quantities, projected central velocity dispersion, σ, measured in km s^{-1}, and mean surface brightness within the r_e isophote, $\langle\mu\rangle$, measured in r_G magnitudes per square arcsec. Data points from left panel are repeated in right panel, but without the error bars. Dashed lines indicate loci of equal absolute magnitudes (within the r_e isophote, in the r_G band), and dotted lines indicate loci of equal log of semimajor axis r_e, measured in h^{-1} pc. A Virgocentric infall model with V_{INF} = 400 km s^{-1} was assumed in computing the absolute luminosities and radii.

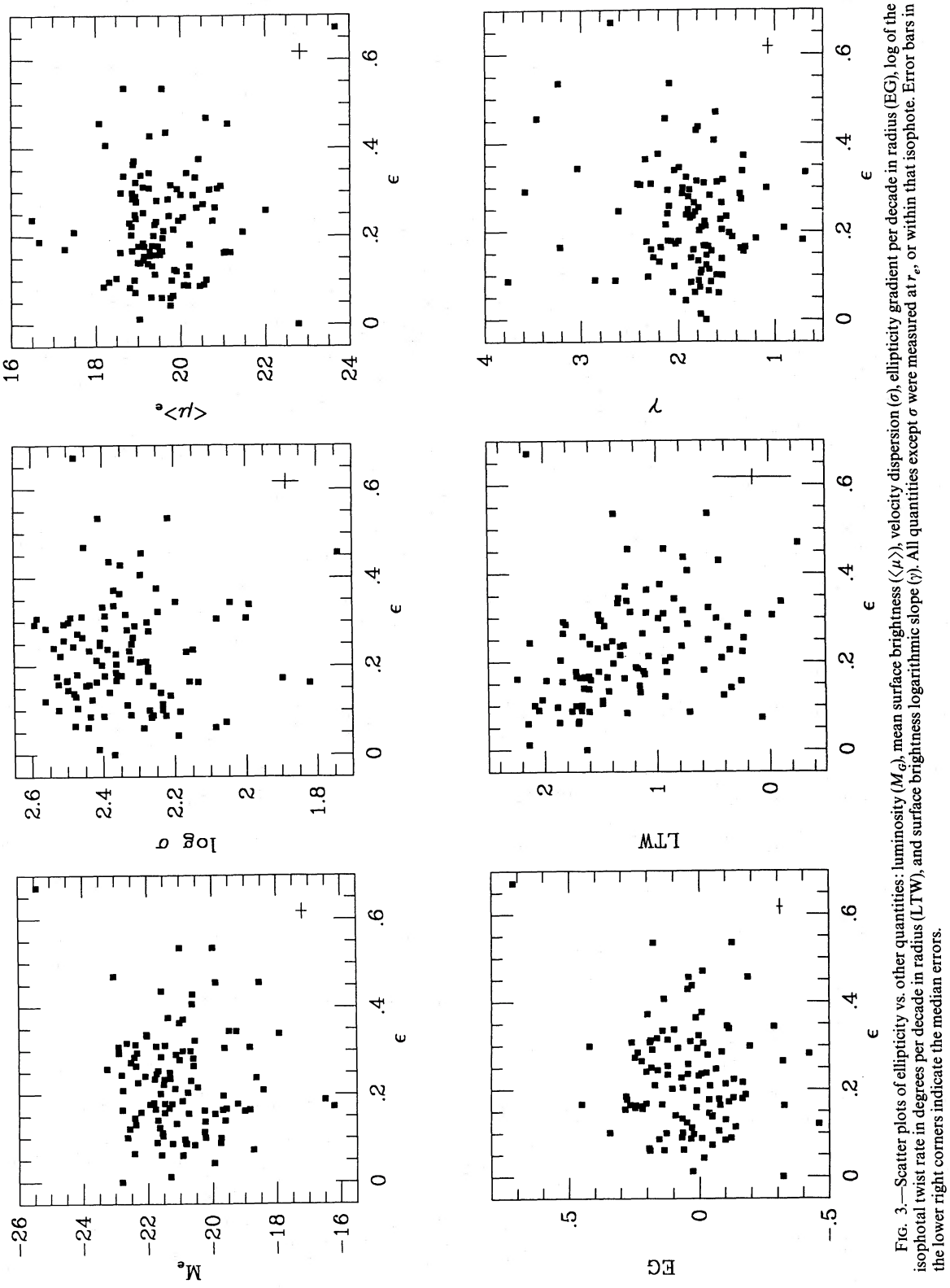

FIG. 3.—Scatter plots of ellipticity vs. other quantities: luminosity (M_e), mean surface brightness ($\langle\mu\rangle$), velocity dispersion (σ), ellipticity gradient per decade in radius (EG), log of the isophotal twist rate in degrees per decade in radius (LTW), and surface brightness logarithmic slope (γ). All quantities except σ were measured at r_e, or within that isophote. Error bars in the lower right corners indicate the median errors.

few percent, or less. The recipe of galaxy formation is very well defined indeed. More refined future measurements may help us to quantify better the intrinsic thickness of the plane, and thus probe directly the "noise" of galaxy formation.

Projected velocity dispersions should be influenced by any dynamical anisotropies that may be present. Such anisotropies give rise to the flattening and/or triaxiality of E galaxies, and thus are reflected in their ellipticities (ϵ), ellipticity gradients, and isophotal twists. Radial-to-tangential anisotropy modifies the radial slope of a surface brightness profile. However, *none* of these shape parameters correlate with velocity dispersion, or any other global property related to the fundamental plane, such as luminosity, surface brightness, etc. Moreover, the shape parameters do *not* correlate between themselves, either. A partial illustration of this fact is given by the scatter plots in Figure 3. The only possible slight correlation is between the ellipticity and the isophotal twist rate, but this may be an artifact: the position angle measurements at small ellipticities become highly uncertain, and large isophotal twists are not to be trusted for $\epsilon < 0.1$. We also find no correlations between any of the structural properties and kinematic variables (maximum rotational velocity, $V_{\max}$, its ratio with the mean velocity dispersion, $V_{\max}/\langle\sigma\rangle$) from a subset of galaxies of Davies *et al.* (1983), except for the known very weak correlation between $V_{\max}$ and ellipticity.

It is of interest to note that the ellipticity does not correlate with either σ or $\langle\mu\rangle$ (Fig. 3). This renders impossible the tests for intrinsic shapes of ellipticals, proposed by several authors in the past : σ and $\langle\mu\rangle$ were expected to correlate with ϵ in the oblate case, and anticorrelate in the prolate case. This clearly does not work, and the only way of distinguishing oblate from prolate elliptical galaxies may be through a detailed mapping of the velocity fields of stars (Davies and Birkinshaw 1986).

There is clearly a variety of forms of the velocity dispersion tensors in ellipticals, but none of these anisotropies, which determine the azimuthal, and to a weaker extent, radial shapes of the distribution of visible light, correlate with the global properties (e.g., mass, luminosity). If such quantities are not related to the properties determined by the fundamental plane, which presumably reflect the process of galaxy formation, we may speculate that they may be related to the properties of the parent *protoclusters*; there are some indications that ellipticities and/or galaxy orientations may be related to the properties of the large-scale structure in which they live (Strom and Strom 1978; Djorgovski 1983, and references therein).

Thus, the elliptical galaxies are a $2 + n$ parameter family, defined by the following observable (projected) quantities: (1) velocity dispersion, (2) surface brightness, and (3), etc., a variety of shape parameters. A possible interpretation in physical terms is that the two principal parameters are the depth of the potential well (1), and the mean density (2), whereas the multitude of subtle dynamical anisotropies (3), etc., determines the details of internal dynamics, and thus the shapes. Note, however, that a full dynamical interpretation of all these observational quantities is afflicted by the projection effects.

A preliminary investigation with a sample of 50 S0 galaxies, but only for 18 of which we have velocity dispersions, shows that they also form a two-dimensional family, and that the equations (tilt) of their fundamental plane are very similar, and possibly identical, to the plane of ellipticals. Their shape parameters also show no correlations between themselves, or with the fundamental plane quantities.

It is is difficult to relate this result directly to the manifold of properties of spirals (e.g., Whitmore 1984; but see also Tully, Mould, and Aaronson 1982), because of very different observables. However, it is certainly possible that the two-dimensionality of a set of fundamental properties is a general property of *all* galaxies, namely, that there is one fundamental relation between size (L, R, or mass), kinematical properties (σ, $V_{\max}$), and density (μ), for *all* galaxies. If so, then the Tully-Fisher relation for spirals and the Faber-Jackson and Kormendy relations for ellipticals (united in our fundamental plane) may be just different aspects of this hypothetical global relation, molded by differences in our observables for galaxies of different morphology. It would be of a considerable interest to check whether the scatter in Tully-Fisher relation is reducible by introduction of a surface brightness term.

Finally, as we already noted, the distribution of light in elliptical galaxies showes a wide variety of shapes, both in azimuthal and radial sense. This means that any realistic dynamical model of elliptical galaxies must incorporate a few structure parameters and reproduce this variety. Worse yet, if ellipticals have substantial amounts of dark material, whose radial and azimuthal distribution is completely unknown at the present, any self-consistent dynamical models, in which stars provide both light and mass, are simply inadequate. It may be possible to augment the existing kinematical and optical surface photometry information with the additional constraints on the true isopotential surfaces from detailed observations of X-ray coronae.

V. THE MASS-TO-LIGHT RATIOS

The presence of dark halos in elliptical galaxies was already indicated by the existence of X-ray coronae (see Forman, Jones, and Tucker 1985). However, in the absence of rotationally supported disks in ellipticals, mapping of the content and distribution of this dark component is rather difficult. In most studies to date, mass-to-light (M/L) ratios have shown a considerable scatter, some of which was (correctly) attributed to the poor and heterogeneous state of photometry at the time.

Following Poveda (1958), we can write for a spherical, isotropic, pure $r^{1/4}$ law galaxy, in which mass follows the light:

$$\frac{M}{L} = 1.55\,\frac{r_e\langle\sigma^2\rangle}{GL}\,, \tag{4}$$

where $\langle\sigma^2\rangle$ is a *mean* observed velocity dispersion within the r_e circle and G is the gravitational constant; everything is measured in cgs units, and both M and L pertain to the half-light radius r_e. The equation (4) can be transformed as

$$\frac{M}{L} = 0.49\,\frac{\langle\sigma^2\rangle}{Gr_e\langle\mathrm{SB}\rangle}\,, \tag{5}$$

where $\langle\mathrm{SB}\rangle$ is the mean surface brightness within the r_e circle. After the substitution of cgs into the solar *red* units and magnitudes, we obtain

$$\log\frac{M}{L} = 2\log\sigma - \log r_e + 0.4\langle\mu\rangle_e - 8.27\,, \tag{6}$$

where σ is in kilometers per second, r_e in parsecs, and $\langle\mu\rangle_e$ in red magnitudes per square arc second (the *blue* M/L ratios will be higher, of course, and a color term should be added). This formula is but a gross approximation: it assumes a spherical galaxy, in which both light and mass follow exactly the $r^{1/4}$ law, and with an isotropic velocity dispersion tensor; all of

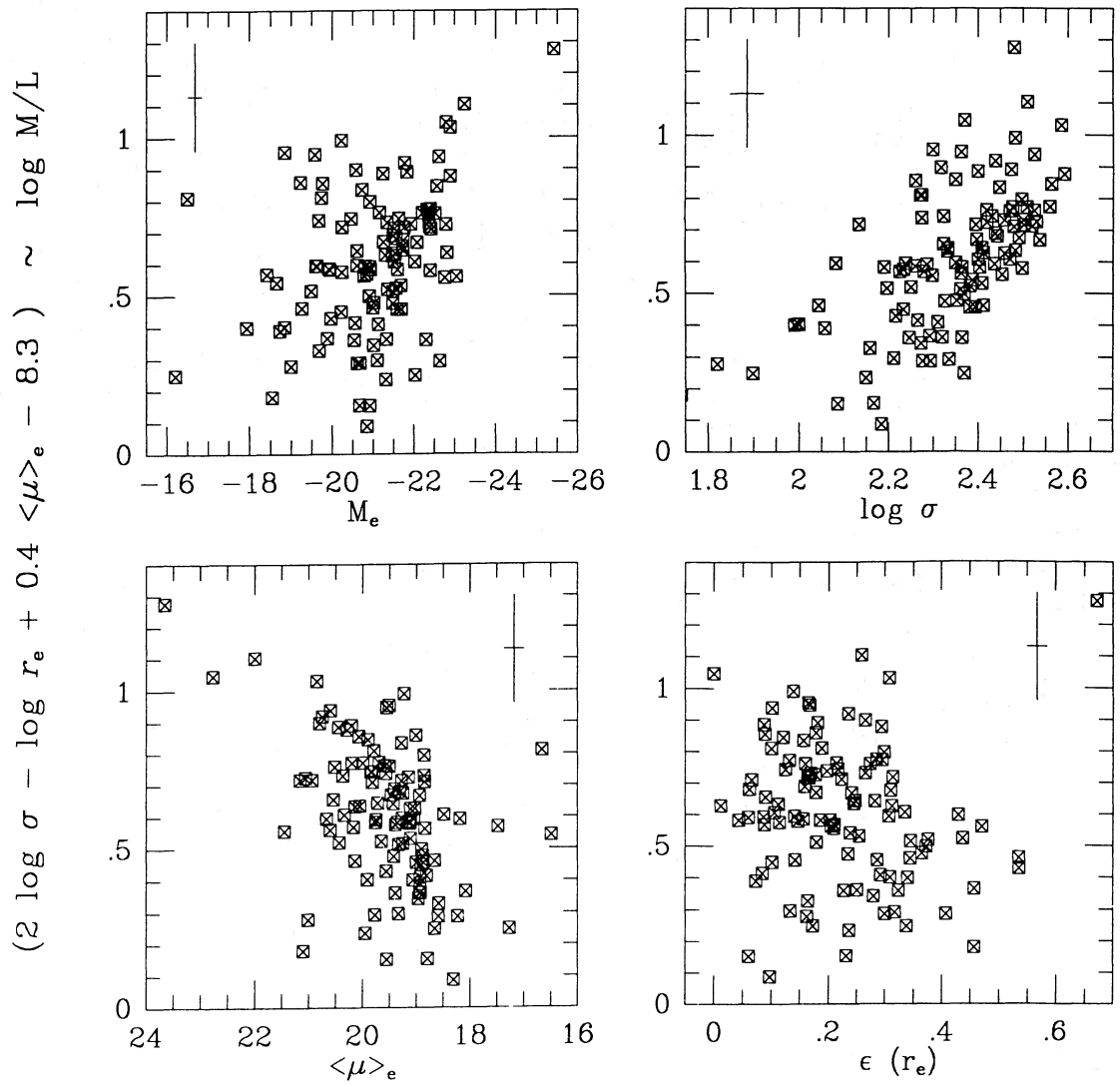

FIG. 4.—M/L ratios, computed as in eq. (6), plotted vs. absolute magnitude (M_e), velocity dispersion (σ), mean surface brightness ($\langle\mu\rangle$), and ellipticity (ϵ). The quantities M_e and $\langle\mu\rangle$ are in the r_G band, within the r_e isophote, and a Virgo infall model with 400 km s^{-1}, and $h = 1$ were used for computation of M_e. Ellipticities are local at r_e, and velocity dispersions are central. Error bars in the corners indicate the median errors. Note the small dynamical range of M/L.

these assumptions are wrong in differing degrees for all real galaxies. Thus, the straight application of such formula (or the equivalent King-Minkowski formula) will inevitably introduce some scatter in the computed M/L ratios. Still, this is the best we can do without detailed measurements of the velocity fields, and a detailed dynamical modeling of individual galaxies.

Figure 4 shows plots of computed M/L ratios versus several other quantities of interest. The only correlation present is with the velocity dispersion, which is a long-known fact (Faber and Jackson 1976, and references therein). This may be expected just from the fact that the velocity dispersion enters as a square in the computation of M/L—in other words, this correlation may be spurious, in part or in whole. The relative constancy of M/L is quite remarkable: a histogram of log (M/L) ratios, measured within the r_e isophote, has a rms of only 0.21 (in log); the median error of measurement is 0.17. This indicates an intrinsic broadening of only $\sim$ 30%, which should also incorporate any differential shape and anisotropy effects, ignored in our simple computation. The M/L changes by certainly much less than a factor of 10 over some four orders of magnitude in luminosity, and may even be constant. However, the peak-to-peak scatter is comparable to that found by Schecter (1980) and Tonry and Davis (1981).

Thus the proportion of the dark and the luminous material in elliptical galaxies is well determined and almost constant, with the median value of $\sim$4.2 (in solar red light units, within the r_e isophote). This relative constancy of M/L ratios may imply that the luminous and the dark matter are well mixed on the scales of galaxies, and larger, *and* that the dissipative process which presumably separated these components operated with equal efficiency everywhere.

VI. CONCLUSIONS

We present here new distance indicator relations for the elliptical galaxies, whose accuracy is at least as good as the Tully-Fisher relation for spirals and may be improved further: the errors of distances predicted with the new relations are currently limited by the measurement errors only, with no discernible intrinsic scatter.

These new relations reflect the presence of a well-defined

plane in the parameter space of photometric and kinematic properties of ellipticals. This "fundamental plane" can be observationally defined as a plane whose axes are velocity dispersion and surface brightness. However, the elliptical galaxies are *not* a two-parameter family, as there are other statistically significant dimensions, viz., the plethora of shape parameters.

We are confronting a problem in which there is a strong regularity in a contrast with a strong cosmic scatter: on one side, there is a set of global properties (luminosity, mass, radius, density, velocity dispersion, metallicity, separately or in various mutual combinations), well described by the thin fundamental plane; the M/L ratios show a very narrow range over a large dynamical range in luminosity, and may even be constant. On the other hand, there is a set of shape parameters (ellipticities, ellipticity gradients, isophotal twists, surface brightness slopes, rotational properties), reflecting internal dynamical structures of ellipticals, all of which are independent from the first family, and generally independent between themselves as well. Any viable theory of galaxy formation will have to explain this situation.

We are indebted to the staff of Lick Observatory for their help during the surface photometry survey, on which this work is based. We acknowledge useful conversations with Sandra Faber, David Burstein, Ivan King, Simon White, Roger Davies, Alan Dressler, and many others, and the stimulating and productive atmosphere of the Hawaii Workshop of 1986. We also thank Brent Tully, the referee, for his constructive comments on the earlier version of this paper. This work was supported in part by the NSF grant AST84-19910 to M. D., and the fellowships from the University of California and Harvard University to S. D.

REFERENCES

Brosche, P. 1973, *Astr. Ap.*, **23**, 259.
Bujarrabal, V., Guibert, J., and Balkowski, C. 1981, *Astr. Ap.*, **104**, 1.
Burstein, D., Davies, R., Dressler, A., Faber, S., Lynden-Bell, D., Terlevich, R., and Wagner, M. 1986, in *Distances to Galaxies and Deviations from the Universal Expansion*, ed. B. Madore and B. Tully (Dordrecht: Reidel), p. 123.
Davies, R., and Birkinshaw, M. 1986, *Ap. J. (Letters)*, **303**, L45.
Davies, R., Efstathiou, G., Fall, M., Illingworth, G., and Schecter, P. 1983, *Ap. J.*, **266**, 41.
de Vaucouleurs, G., and Olson, D. 1982, *Ap. J.*, **256**, 346.
Djorgovski, S. 1983, *Ap. J. (Letters)*, **274**, L7.
———. 1985*a*, Ph.D. thesis, University of California, Berkeley.
———. 1985*b*, *Pub. A.S.P.*, **97**, 1119.
Djorgovski, S., and Davis, M. 1986, in *Distances to Galaxies and Deviations from the Universal Expansion*, ed. B. Madore and B. Tully (Dordrecht: Reidel), p. 135.
Djorgovski, S., Davis, M., and Kent, S. 1985, in *Lecture Notes in Physics*, Vol. **232**, *New Aspects of Galaxy Photometry*, ed. J.-L. Nieto (Berlin: Springer-Verlag), p. 257.
Dressler, A., Lynden-Bell, D., Burstein, D., Davies, R., Faber, S., Wagner, M., and Terlevich, R. 1986, *Ap. J.*, **313**, 42.
Efstathiou, G., and Fall, M. 1984, *M.N.R.A.S.*, **206**, 453.
Faber, S., and Jackson, R. 1976, *Ap. J.*, **204**, 668.
Forman, W., Jones, C., and Tucker, W. 1985, *Ap. J.*, **293**, 102.
Huchra, J. 1985, in *Proc. ESO Conf. and Workshop No. 20, The Virgo Cluster of Galaxies*, ed. O.-G. Richter and B. Binggeli (Munich: ESO), p. 181.
Kormendy, J. 1982, in *Proc. 12th Saas-Fe Advanced Course Morphology and Dynamics of Galaxies* (Geneva Obs. Pub.).
———. 1985, *Ap. J.*, **295**, 73.
Kraan-Korteweg, R. 1983, *Astr. Ap.*, **125**, 109.
Lauer, T. 1985, *Ap., J.*, **292**, 104.
Meiksin, A. 1985, private communication.
Petrosian, V. 1976, *Ap. J. (Letters)*, **209**, L1.
Poveda, A. 1958, *Bol. Obs. Tonantzitla Tacubaya*, **17**, 3.
Sandage, A., Binggeli, B., and Tamman, G. 1985, *A.J.*, **90**, 1759.
Schechter, P. 1980, *A.J.*, **85**, 801.
Strom, S., and Strom, K. 1978, *A.J.*, **83**, 732.
Terlevich, R., Davies, R., Faber, S., and Burstein, D. 1981, *M.N.R.A.S.*, **196**, 381.
Tonry, J., and Davis, M. 1981, *Ap. J.*, **246**, 666.
Tully, R. B., Mould, J., and Aaronson, M. 1982, *Ap. J.*, **257**, 527.
Watanabe, M., Kodaira, K., and Okamura, S. 1985, *Ap. J.*, **292**, 72.
Whitmore, B. 1984, *Ap. J.*, **278**, 61.
Whitmore, B., McElroy, D., and Tonry, J. 1985, *Ap. J. Suppl.*, **59**, 1.
Wirth, A., and Gallagher, J. 1984, *Ap. J.*, **282**, 85.

M. Davis: Astronomy Department, University of California, Berkeley, CA 94720

S. Djorgovski: Center for Astrophysics, 60 Garden St., Cambridge, MA 02138